Does Extratropical Transition Impact Tornado Production in Tropical Cyclones?

NEIL CROSBY*

National Weather Center Research Experiences for Undergraduates Program
Norman, Oklahoma
Jackson State University
Jackson, MS

BENJAMIN A. SCHENKEL

Cooperative Institute for Mesoscale Meteorological Studies, University of Oklahoma
Norman, Oklahoma

ABSTRACT

The conditions favoring tropical cyclone (TC) tornadoes are likely also present during extratropical transition (ET) including strong ambient deep-tropospheric vertical wind shear, sufficient convective-scale lower-tropospheric vertical wind shear, and thermodynamic instability, and supercellular convection. However, no previous studies have investigated how ET tornado occurrence may differ from the remainder of the TC lifespan. Hence, our objective is to investigate differences in tornado frequency and location between ET and non-ET TCs using tornado data, TC track data, and reanalysis-derived cyclone phase space data. These results showed that ET does increase 6-h tornado frequency compared to non-ET TCs. However, there was no change in the frequency of damaging tornadoes in ET versus non-ET cases. Regarding location, we found that tornadoes in ET cases are mostly confined to the U.S. east coast, while TC tornadoes widely occur in the southern U.S. These results are also consistent with the location of ET and non-ET TCs. Together, this research will provide the foundation for improving tornado forecasts in landfalling ET cases.

1. Introduction

Our current knowledge of tropical cyclone (TC) tornado frequency and location remains incomplete (Edwards 2012). Specifically, there have been no prior studies of tornadoes during extratropical transition (ET). ET is defined as the process by which a TC becomes an extratropical cyclone, which is characterized by the cyclone transitioning from a non-frontal, warm-core cyclone to a frontal, cold-core cyclone (Jones and Coauthors 2003; Evans et al. 2017). Approximately, 50% of all TCs and 50% of landfalling TCs eventually undergo ET (Hart and Evans 2001; Bieli et al. 2019), which suggests that at least some tornadoes occur during ET. Hence, this study will examine how ET influences tornado occurrence.

To understand how tornado occurrence may change during ET, it is necessary to recall the characteristics of TC supercells and their environments. Typically, TC supercells are "miniature" supercells, which are characterized by weaker updrafts, shorter lifespans, shallower vertical depth, and smaller horizontal scale (Spratt et al. 1997; Eastin and Link 2009). TC tornadoes and their attendant supercells often occur in environments characterized by sufficient thermodynamic instability and strong vertical wind shear in the lower troposphere (McCaul Jr. 1991; Edwards 2012). These characteristics are attributed to several factors including: enhanced surface friction over land, the warm-core structure of the TC, enhanced frontogenesis due to TC-baroclinic zone interactions, and diurnal surface heating (Novlan and Gray 1974; Gentry 1983; McCaul Jr. 1991; Knupp et al. 2006). More recent work has also shown that ambient deep-tropospheric (i.e., 850–200-hPa layer) vertical wind shear (VWS) is a key factor influencing TC tornado frequency and location (Schenkel et al. 2020). Specifically, Schenkel et al. (2020) has shown that stronger VWS is associated with enhanced tornado production and an increased concentration of tornadoes in the downshear sector of the TC (i.e., half of TC in direction of VWS vector). VWS creates favorable tornadic environments in the downshear sector likely due to: 1) constructive superposition between the TC and ambient winds, and 2) VWS-induced enhancement of the primary and secondary circulation of the TC (Jones 1995; Reasor et al. 2004; Schenkel et al. 2020).

The importance of these aforementioned factors on tornado production may be altered during ET. Despite the

* *Corresponding author address:* Neil Crosby, Jackson State University, 1400 John R. Lynch St, Jackson, MS 39217
E-mail: ncrosby97@gmail.com

typical weakening of the TC, ET cases may also be associated with favorable kinematic and thermodynamic environments including strong VWS, the transition to cold-core cyclone structure, and the development of strong temperature and moisture gradients as the TC becomes embedded in a baroclinic zone (Hart 2003; Evans et al. 2017). More specifically, the influence of VWS on ET causes intensification of convection in the downshear region in response to the vertical tilting of the TC by VWS (Jones 1995; Evans et al. 2017). In particular, a case study of Typhoon Sinlaku (2008) (Foerster et al. 2014) showed that the location of inner-core deep convection was most likely the result of strong VWS during the early stages of ET with cells initiating downshear right, reaching peak amplitude downshear left, and weakening upshear (Foerster et al. 2014; Quinting et al. 2014). Also, winds will increase with height above the boundary layer as the cyclone transitions from warm-core to cold-core (Hart 2003; Jones et al. 2003). Deep convection also still occurs in the latter stages of transition and is confined to the northwest quadrant of the storm associated with strong ascent within the eyewall (Klein et al. 2000; Ritchie and Elsberry 2001). The extra source of lift provided by baroclinic boundaries encountered during ET may also intensify or maintain convective activity (Klein et al. 2000; Ritchie and Elsberry 2001). Lastly, in the final stage of ET, the structural evolution of the storm reaches completion, and the storm may dissipate, merge with another extratropical cyclone, or re-intensify, depending on the given environment (Klein et al. 2000; Evans et al. 2017). At this stage, we may expect tornadoes to initiate in the warm sector of newly transitioned extratropical cyclone (Klein et al. 2000; Evans et al. 2017)

The structural changes that occur to TCs during ET motivate an examination of tornadoes, especially since none currently exist. Hence, the objective of this study is to investigate how ET may impact tornado frequency and location for comparison with non-ET TCs. Specifically, this study will analyze how the frequency, geographic location, and TC-relative distance of tornadoes differ between ET and non-ET TCs. Our analysis will primarily use multidecadal tornado and TC data together with objectively-defined ET start and end times using the cyclone phase space. This work may have the potential to provide forecasters with a foundation for more accurate predictions of TC tornadoes.

2. Data and methods

a. TC tornado data

Observed TC tornado data is obtained from the Storm Prediction Center (SPC) TCTOR dataset (Edwards 2010), which provides tornado track and damage data for cases associated with TCs. TCTOR data is available from 1995–2019 to coincide with improvements in radar detection from the WSR-88D radar network and the development of modern verification practices (Edwards 2010). Individual tornado reports from the dataset are subjectively analyzed by SPC forecasters for association with TCs.

b. TC track and intensity data

Observed TC track data is taken from the National Hurricane Center HURricane DATa, 2nd generation (HURDAT2). This dataset provides 6-h track and intensity data from 1995–2019 (Landsea and Franklin 2013). For a TC to be considered capable of producing a tornado, the TC must be within 750 km of the U.S. coast (Schenkel et al. 2020). Instead of analyzing the tornado production throughout the lifespan of individual TCs, our focus will be on the 6-h frequency of tornadoes. Our focus will be on the latter for two reasons: 1) TC track data is provided in 6-h intervals and 2) environments change quickly over the lifespan of a TC due to various factors including VWS (Rios-Berrios et al. 2016a,b; Nguyen et al. 2017; Ryglicki et al. 2018) and land interaction (Emanuel 1986; Kaplan and DeMaria 1995; DeMaria et al. 2005).

c. ET Classification

ET start and end times will be defined using the cyclone phase space (CPS; Hart 2003) applied to data from the European Center for Medium-Range Weather Forecasts (ECMWF) 5th generation reanalysis (ERA-5) (Hersbach et al. 2020). The cyclone phase space consists of two parameters. The first is the lower-tropospheric thermal asymmetry parameter (i.e., B parameter), which quantifies the difference between 900–600-hPa geopotential layer thickness to the left-and-right-of TC motion (Hart 2003; Evans and Hart 2003). A B parameter value greater than 10 m (i.e., empirically defined) indicates that a cyclone is beginning to develop lower-tropospheric frontal structure, which defines the start of ET (Hart 2003; Evans and Hart 2003). The second parameter is the lower-tropospheric thermal wind parameter, which quantifies the change in the horizontal geopotential height gradient with height between 900 and 600 hPa (Hart 2003; Evans and Hart 2003). A negative thermal wind parameter marks the end of ET, as the cyclone has transitioned from being warm core to cold core (Hart 2003; Evans and Hart 2003). In the present study, we categorize all 6-h times for TCs that do not undergo ET or have yet to complete ET as non-ET cases. The 6-h TC times during ET are defined as ET cases.

3. Results

Our analysis will first examine how tornado frequency varies between ET and non-ET TCs. The second part of our analysis will focus on the location of tornadoes between these two subsets of cases.

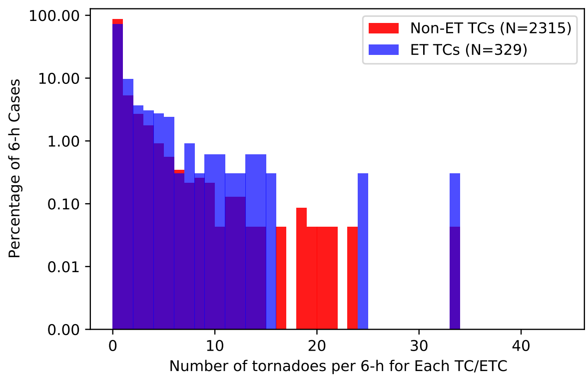

FIG. 1. Bar plot 6-h tornado frequency (%) for ET and non-ET TCs. The percentage is computed relative to the total number of 6-h cases in each subset. The number of total 6-h cases in each subset is given in the legend.

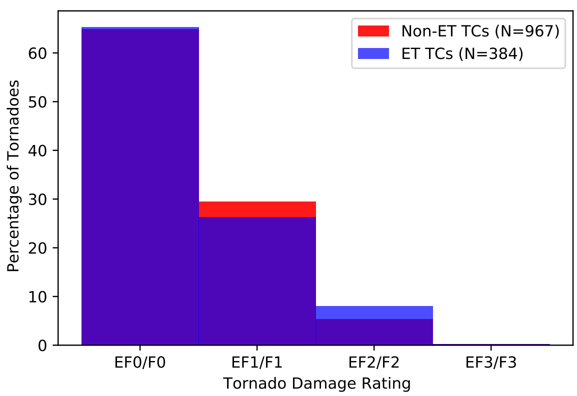

FIG. 2. Bar plot tornado damage category (%) for tornadoes during ET and non-ET TCs. The percentage is computed relative to the total number of tornadoes in each subset. The number of total tornadoes in each subset is given in the legend.

a. Tornado frequency

Although a TC may begin to weaken, it still has the potential for substantial tornado production during ET. The histogram plot in Fig. 1 quantifies the differences in 6-h tornado frequency during ET and non-ET TCs. Figure 1 shows that both ET and TC cases typically produce 0–1 tornadoes per 6-h period. However, 6-h times during ET typically have more tornadoes compared to non-ET cases, especially for large numbers of tornadoes (i.e., $\geq$10 tornadoes). One hypothesis for the increase in tornado production may be due to the more frequent presence of baroclinic boundaries in ET cases, which may strengthen convection by providing a focus for convection alongside the presence of strong VWS (Evans et al. 2017; Schenkel et al. 2020). The legend of this figure also shows the total number of 6-h times in each subset for TCs within 750 km of the U.S. coast. ET events constitute 12% of all 6-h times within 750 km of the coast. This small percentage is likely attributable to: 1) approximately 50% of TCs undergoing ET (Hart and Grumm 2001; Bieli et al. 2019) and 2) ET lasting 24–36 hours, whereas TCs typically last, on average, 5 days (Klein et al. 2000; Ritchie and Elsberry 2001; Evans and Hart 2003; Schenkel and Hart 2012).

Figure 2 shows tornado damage rating stratified by the non-ET and ET TCs. There are little to no differences between damage categories between the two subsets. In conjunction with the results regarding tornado frequency, this may suggest that ET environments become more favorable for tornadoes, but not necessarily supportive of more damaging events. The legend of this figure also shows the total number of tornadoes in the ET and non-ET subset. Approximately 28% of TC tornadoes occur during ET cases. Again, the smaller percentage may be due to the short period of ET for most TCs compared to the rest of their life span (Klein et al. 2000; Ritchie and Elsberry 2001; Evans and Hart 2003).

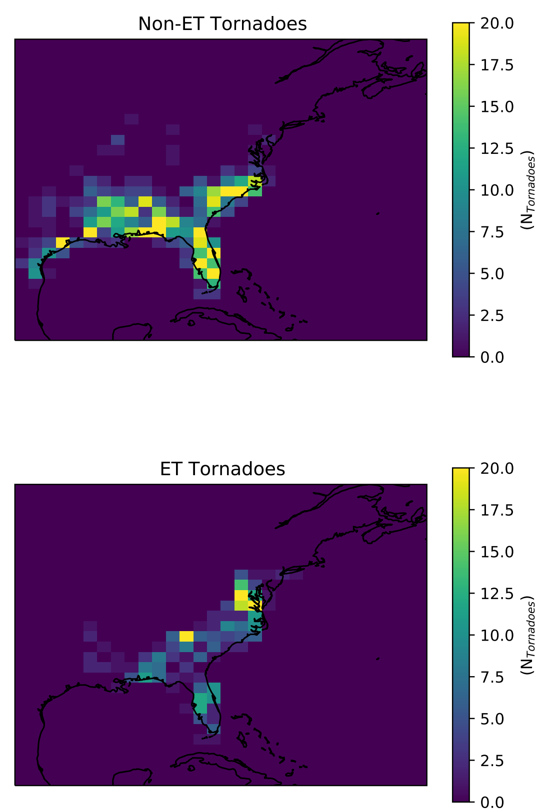

FIG. 3. Map view of tornado location in (top) non-ET and (bottom) ET cases.

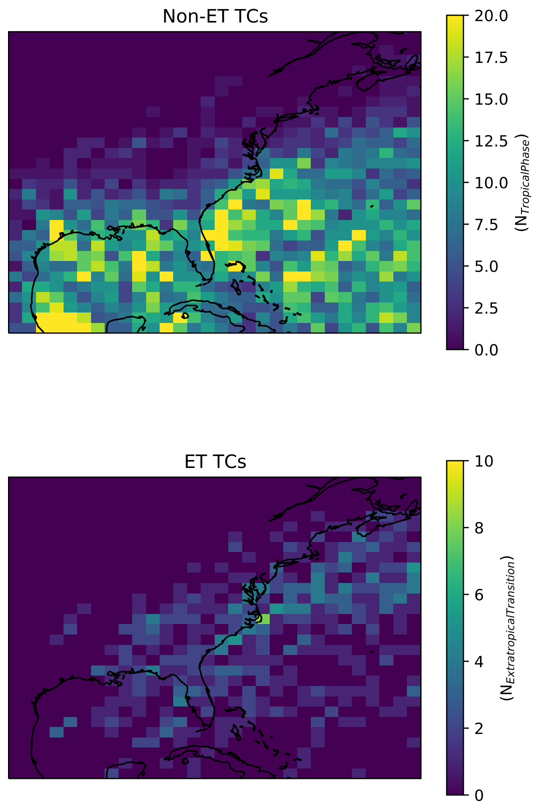

FIG. 4. As in Fig. 3, but for 6-h TC track points.

b. Tornado geographical location

ET and non-ET tornadoes occur in similar geographical locations, with some crucial differences. Figure 3 displays a two-dimensional map view histogram of tornado location for ET and non-ET TCs. Figure 3 shows that non-ET tornadoes are distributed over a large portion of the south and the southeast U.S. with a maximum in Florida, the Gulf Coast, and the Carolinas. In contrast, ET tornadoes are confined to the U.S. east coast with a maximum in the Mid-Atlantic region.

Next, Fig. 4 displays the location of all 6-h ET and non-ET cases. We see that ET occurrences are much fewer and further east than non-ET cases. Specifically, ET case frequency maximizes around the mid-Atlantic region similar to prior work (Hart and Evans 2001; Bieli et al. 2019), which is broadly consistent with tornado location (Fig. 3). Non-ET cases, however, are located much farther south and west, being particularly concentrated in the Gulf of Mexico, in which there are very few ET cases. These location differences may be partly attributed to: 1) the presence of baroclinic boundaries along the east coast favoring ET cases and 2) higher SSTs in the Gulf of Mexico favoring non-ET cases.

c. Tornado cyclone-relative location

The TC-relative radial distance of tornadoes is shown next in Fig. 5. The distances of tornadoes from the TC center in ET (i.e., 100–500 km from storm center) are less concentrated than non-ET cases (i.e., 200–400 km) (McCaul Jr. 1991; Schultz and Cecil 2009). (Evans et al. 2017). However, these differences in the radial distance of tornadoes between the two subsets are marginal suggesting that ET has marginal impacts.

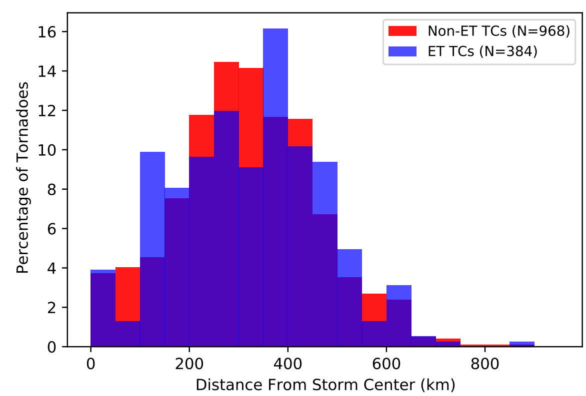

FIG. 5. Bar plot of radial distance of tornadoes from cyclone center (%) for tornadoes in non-ET and ET TCs. The percentage is computed relative to the total number of tornadoes in each subset

4. Summary and discussion

This study aimed to quantify the differences in tornado frequency and location during the ET and non-ET TCs. Our analysis primarily used observed tornado and TC data together with reanalysis-derived cyclone phase space data. Using this data, we analyzed 6-h tornado frequency, TC-relative radial distance, damage rating, and geographic location for each subset.

Our analysis firstly revealed that ET cases tend to produce more tornadoes per 6-h period than TCs. Moreover, ET TCs produce approximately 30% of TC tornadoes. However, there were practically no differences in the damage rating of tornadoes between the two subsets.

Substantial differences in the geographic location of tornadoes between non-ET and ET cases were also shown. Specifically, ET tornadoes are located almost strictly along the east coast. In contrast, non-ET tornadoes were concentrated in the southern U.S., along the Gulf Coast, and even Texas. These results are broadly consistent with the expected locations based on differences in non-ET and ET

TC tracks. Last, there was found to be virtually no difference in radial distances of tornadoes from the cyclone center between non-ET and ET cases.

In closure, the results confirm that ET has noticeable impacts on tornado production – specifically, tornado frequency and geographic location. This study serves as a basis for beginning to understand: 1) differences in tornado occurrence between ET and non-ET TCs and 2) which ET characteristics (e.g., baroclinic boundaries) lead to these differences in tornado occurrence. Such information is crucial given that TC tornado forecasts are less skillful at all lead times compared to Great Plains cases (Edwards 2012; Martinaitis 2017). Future work will further investigate how ET impacts TC tornado occurrence including case studies, as well as the impacts of strong and weak VWS on tornado production during ET cases.

References

Bieli, M., S. J. Camargo, A. H. Sobel, J. L. Evans, and T. Hall, 2019: A global climatology of extratropical transition. Part I: Characteristics across basins. *J. Climate*, **32**, 3557–3582.

DeMaria, M., M. Mainelli, L. K. Shay, J. A. Knaff, and J. Kaplan, 2005: Further improvements to the Statistical Hurricane Intensity Prediction Scheme (SHIPS). *Wea. Forecasting*, **20**, 531–543.

Eastin, M. D., and M. C. Link, 2009: Miniature supercells in an offshore outer rainband of Hurricane Ivan (2004). *Mon. Wea. Rev.*, **137**, 2081–2104.

Edwards, R., 2010: Tropical cyclone tornado records for the modernized National Weather Service era. *Proc., 25th Conf. on Severe Local Storms*, Denver, CO, Amer. Meteor. Soc., P3.1.

Edwards, R., 2012: Tropical cyclone tornadoes: A review of knowledge in research and prediction. *Electron. J. Severe Storms Meteor.*, **7**, 1–61.

Emanuel, K., 1986: An air-sea interaction theory for tropical cyclones. Part I: Steady-state maintenance. *J. Atmos. Sci.*, **43**, 585–604.

Evans, C., and Coauthors, 2017: The extratropical transition of tropical cyclones. Part I: Cyclone evolution and direct impacts. *Mon. Wea. Rev.*, **145**, 4317–4344.

Evans, J., and R. Hart, 2003: Objective indicators of the life cycle evolution of extratropical transition for Atlantic tropical cyclones. *Mon. Wea. Rev.*, **131**, 909–925.

Foerster, A. M., M. M. Bell, P. A. Harr, and S. C. Jones, 2014: Observations of the eyewall structure of Typhoon Sinlaku (2008) during the transformation stage of extratropical transition. *Mon. Wea. Rev.*, **142**, 3372–3392.

Gentry, R. C., 1983: Genesis of tornadoes associated with hurricanes. *Mon. Wea. Rev.*, **111**, 1793–1805.

Hart, R., 2003: A cyclone phase space derived from thermal wind and thermal asymmetry. *Mon. Wea. Rev.*, **131**, 585–616.

Hart, R., and J. Evans, 2001: A climatology of the extratropical transition of Atlantic tropical cyclones. *J. Climate*, **14**, 546–564.

Hart, R., and R. Grumm, 2001: Using normalized climatological anomalies to rank synoptic-scale events objectively. *Mon. Wea. Rev.*, **129**, 2426–2442.

Hersbach, H., and Coauthors, 2020: The ERA5 global reanalysis. *Quart. J. Roy. Meteor. Soc.*, in press.

Jones, S., 1995: The evolution of vortices in vertical shear. Part I: Initially barotropic vortices. *Quart. J. Roy. Meteor. Soc.*, **121**, 821–851.

Jones, S., and Coauthors, 2003: ET, THORPEX, and the North Atlantic TrEC. *Second International Workshop on extratropical transition*, Halifax, NS, Canada, Environment Canada.

Jones, S. C., and Coauthors, 2003: The extratropical transition of tropical cyclones: Forecast challenges, current understanding, and future directions. *Wea. Forecasting*, **18**, 1052–1092.

Kaplan, J., and M. DeMaria, 1995: A simple empirical model for predicting the decay of tropical cyclone winds after landfall. *J. Appl. Meteor. Climatol.*, **34**, 2499–2512.

Klein, P., P. Harr, and R. Elsberry, 2000: Extratropical transition of western North Pacific tropical cyclones: An overview and conceptual model of the transformation stage. *Wea. Forecasting*, **15**, 373–395.

Knupp, K. R., J. Walters, and M. Biggerstaff, 2006: Doppler profiler and radar observations of boundary layer variability during the landfall of Tropical Storm Gabrielle. *J. Atmos. Sci.*, **63**, 234–251.

Landsea, C. W., and J. L. Franklin, 2013: Atlantic hurricane database uncertainty and presentation of a new database format. *Mon. Wea. Rev.*, **141**, 3576–3592.

Martinaitis, S. M., 2017: Radar observations of tornado-warned convection associated with tropical cyclones over Florida. *Wea. Forecasting*, **32**, 165–186.

McCaul Jr., E. W., 1991: Buoyancy and shear characteristics of hurricane-tornado environments. *Mon. Wea. Rev.*, **119**, 1954–1978.

Nguyen, L. T., R. F. Rogers, and P. D. Reasor, 2017: Thermodynamic and kinematic influences on precipitation symmetry in sheared tropical cyclones: Bertha and Cristobal (2014). *Mon. Wea. Rev.*, **145**, 4423–4446.

Novlan, D. J., and W. M. Gray, 1974: Hurricane-spawned tornadoes. *Mon. Wea. Rev.*, **102**, 476–488.

Quinting, J. F., M. M. Bell, P. A. Harr, and S. C. Jones, 2014: Structural characteristics of T-PARC Typhoon Sinlaku during its extratropical transition. *Mon. Wea. Rev.*, **142**, 1945–1961.

Reasor, P., M. Montgomery, and L. Grasso, 2004: A new look at the problem of tropical cyclones in vertical shear flow: Vortex resiliency. *J. Atmos. Sci.*, **61**, 3–22.

Rios-Berrios, R., R. D. Torn, and C. A. Davis, 2016a: An ensemble approach to investigate tropical cyclone intensification in sheared environments. Part I: Katia (2011). *J. Atmos. Sci.*, **73**, 71–93.

Rios-Berrios, R., R. D. Torn, and C. A. Davis, 2016b: An ensemble approach to investigate tropical cyclone intensification in sheared environments. Part II: Ophelia (2011). *J. Atmos. Sci.*, **73**, 1555–1575.

Ritchie, E. A., and R. L. Elsberry, 2001: Simulations of the transformation stage of the extratropical transition of tropical cyclones. *Mon. Wea. Rev.*, **129**, 1462–1480.

Ryglicki, D. R., J. H. Cossuth, D. Hodyss, and J. D. Doyle, 2018: The unexpected rapid intensification of tropical cyclones in moderate vertical wind shear. Part I: Overview and observations. *Mon. Wea. Rev.*, **146**, 3773–3800.

Schenkel, B., R. Edwards, and M. Coniglio, 2020: A climatological analysis of ambient deep-tropospheric vertical wind shear impacts upon tornadic supercells in tropical cyclones. *Wea. Forecasting*, accepted.

Schenkel, B., and R. Hart, 2012: An examination of tropical cyclone position, intensity, and intensity life cycle within atmospheric reanalysis datasets. *J. Climate*, **25**, 3453–3475.

Schultz, L. A., and D. J. Cecil, 2009: Tropical cyclone tornadoes, 1950–2007. *Mon. Wea. Rev.*, **137**, 3471–3484.

Spratt, S. M., D. W. Sharp, P. Welsh, A. Sandrik, F. Alsheimer, and C. Paxton, 1997: A WSR-88D assessment of tropical cyclone outer rainband tornadoes. *Wea. Forecasting*, **12**, 479–501.